IVS Memorandum 2008-013v01

14 August 2008

"Investigation of the Impact of Random Error Sources on Position Repeatability using the VLBI2010 PPP Simulator"

Andrea Pany, Jörg Wresnik, Johannes Böhm

Investigation on the Impact of Random Error Sources on Position Repeatability using the VLBI2010 PPP Simulator

A. Pany, J. Wresnik, J. Böhm

Abstract
The main random error sources in VLBI are troposphere, station clock and thermal noise of the receiving system. These error sources are considered when generating artificial group delay observables for VLBI2010 simulations. In this memo, the impact of these three error sources on results of the VLBI2010 PPP simulations are presented. After a brief introduction in Section 1, Section 2 deals with the most limiting factor in VLBI analysis, namely the troposphere. It is shown, how the parameters driving the turbulence impact on the estimation of station position. In Section 3, simulations with six different clocks are performed to show the impact of clock accuracy on the estimation of station position with PPP. Section 4 finally deals with the contribution of the thermal noise.

1. Introduction

For VLBI2010 PPP simulations artificial group delay observables $delay_{group}$ are generated as

$$delay_{group} = zwd \cdot mfw(el) + clk + wn$$

with *zwd* being the equivalent zenith wet delay (provided by a turbulence model), *mfw* the wet mapping function (considered to be free of error), *el* the elevation angle, *clk* the stochastic variations of station clock and *wn* white noise accounting for the thermal noise of the receiving system. The fake delay observables are generated for 25 identical 24-hour sessions using different sets of random numbers.
Former investigations (Wresnik et al. 2007) have shown that the troposphere is the most limiting factor in VLBI analysis. For VLBI2010 simulations, the equivalent zenith wet delay is provided by a turbulence model (Nilsson et al. 2007). The parameters driving the turbulence are the refractive index strucure constant C_n, the effective height of wet troposphere H, and the wind velocity v, the variability of the artificial zenith wet delay thus being determined by the combination of these three parameters. The stochastic variations of station clock are determined by the Allan standard deviation (ASD) used for the generation of the clock time series (Böhm et al. 2007).
To assess the impact of all of these parameters and of the whithe noise term in (1) on position estimates with PPP, simulation studies were carried out for which only one parameter at a time was varied and the others were held constant. The Kalman filter version of the PPP software was used (Pany et al. 2008). The troposphere was modeled with a zenith wet delay and superimposed gradients, all estimated as random walks with variance rates of 0.7 and 0.5 ps²/s respectively. Clock parameters estimated were a rate (deterministic) and a random walk offset (variance rate 1 ps²/s). Coordinate residuals were estimated as deterministic parameters.

2. Impact of the turbulence parameters

It is important to gain knowledge about how the parameters driving the turbulence impact on position accuracy. With a Monte Carlo simulator this is straightforward to do. The analysis was performed for schedule st16uni_60_12_230X_0_0.skd, a VLBI2010 16 station test schedule with uniform sky coverage over 12 min intervals while switching every 60 s (for more details about this type of schedule see Petrachenko et al. 2008). The clock accuracy was set to an ASD of 1e-14 @ 50 min, and a white noise of 4/sqrt(2) ps was used.

When not being varied, the turbulence parameters were set to the following values: C_n = 1.0e-7 $m^{-1/3}$, H = 2000 m, v = 10 m/s towards East. The turbulent equivalent zenith wet delays were generated using the same turbulence parameters for all stations.

2.1 Varying the refractive index structure constant C_n

The impact of C_n on 3D position accuracy can be seen in Figure 1. It shows bar plots of rms of 3D position error about the true value for C_n values of 0.5e-7 (blue), 1.0e-7 (green) and 2.0e-7 (red) $m^{-1/3}$. For troposphere height H and wind velocity v the standard values given above were kept. It can be seen that the choice of C_n has a significant impact on position accuracy.

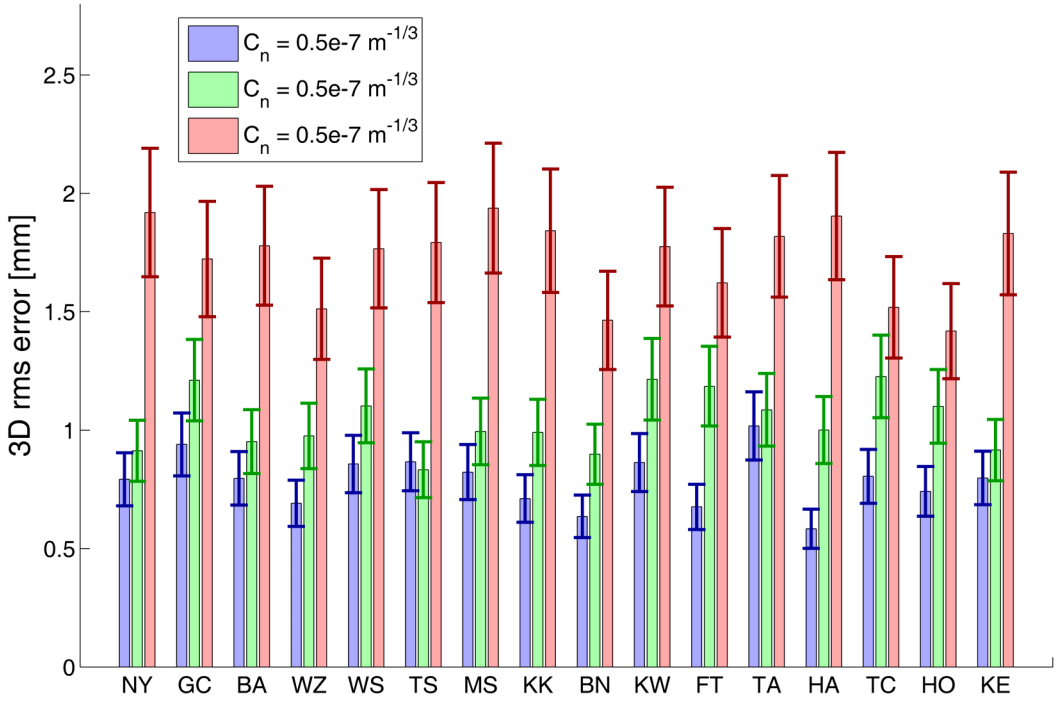

Figure 1: 3D rms error about the true value in mm for three different C_n values. H = 2000 m, v = 10 m/s, wind blowing towards East. For the generation of the turbulent equivalent zenith wet delays the same parameters were used for all stations. Error bars: rms/sqrt(2n), where n = 25. Schedule: st16uni_60_12_230X.skd, ASD 1e-14 @ 50 min, wn = 4/sqrt(2) ps.

Table 1: median rms of 3D position error, Up, North, and East component for different C_n values. H = 2000 m, v = 10 m/s, wind blowing towards East. Schedule_st16uni_60_12_230X.skd, ASD 1e-14 @ 50 min, wn = 4/sqrt(2) ps.

		C_n = 0.5e-7 $m^{-1/3}$	C_n = 1.0e-7 $m^{-1/3}$	C_n = 2.0e-7 $m^{-1/3}$
median rms error [mm]	3D	0.8	1.0	1.8
	Up	0.8	0.9	1.7
	North	0.2	0.3	0.4
	East	0.2	0.2	0.3

In Table 1 the median 3D rms errors are given. These values are plotted versus C_n in Figure 2. The error bars show the 16th and 84th percentile, corresponding to 1 sigma about the median.

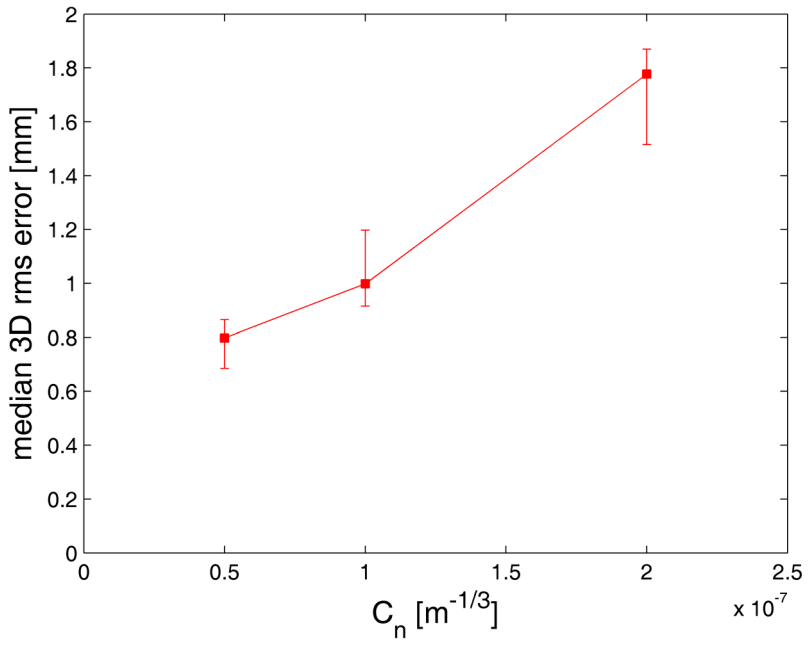

Figure 2: median 3D rms error [mm] versus refractive index structure constant C_n. The errorbars show the 16th and 84th percentile, corresponding to 1 sigma about the median. H = 2000 m, v = 10 m/s.

With the PPP Simulator, in contrast to the simulators based on the VLBI analysis softwares OCCAM and Calc/Solve, it is possible to perform such investigations for single stations, making it possible to test many values in short time. Thus, a second investigation of this kind was carried out. For two uniform sky schedules (st16uni_60_12_230X.skd and st16uni_30_6_230X.skd) one station was picked (Wettzell) to be used as reference station, i.e. time epoch, azimuth and elevation of observations of Wettzell were used for the generation of fake delay observables. The turbulence parameters were varied according to the following specifications:

C_n: 0.5, 1.0, 1.5, 2.0, 2.5, 3.0, 3.5 e-7 [$m^{-1/3}$]
H: 500, 1000, 1500, 2000, 2500, 3000, 3500, 4000 [m]
v: 7, 15 [m/s] towards North-East

For this investigation, 250 repetitions were carried out (in contrast to the first investigation presented here, for which 25 runs were performed as usual for VLBI2010 simulation studies).

Figure 3 presents rms of 3D position error about the true value in mm versus refractive index structure constant C_n for different troposphere heights H. The wind speed was chosen to be 7 m/s,

the wind was blowing towards North-East. The error bars show 1 sigma of the rms scatter, i.e. rms/sqrt(2n), where n is the number of repetitions (250). From Figure 3 it can be deduced that the dependence of rms of 3D position error on the refractive index structure constant is almost linear. Comparing results for different heights H, it can be seen that the troposphere height has an impact on the slope of the lines, i.e. the greater H, the greater the slope of the line.

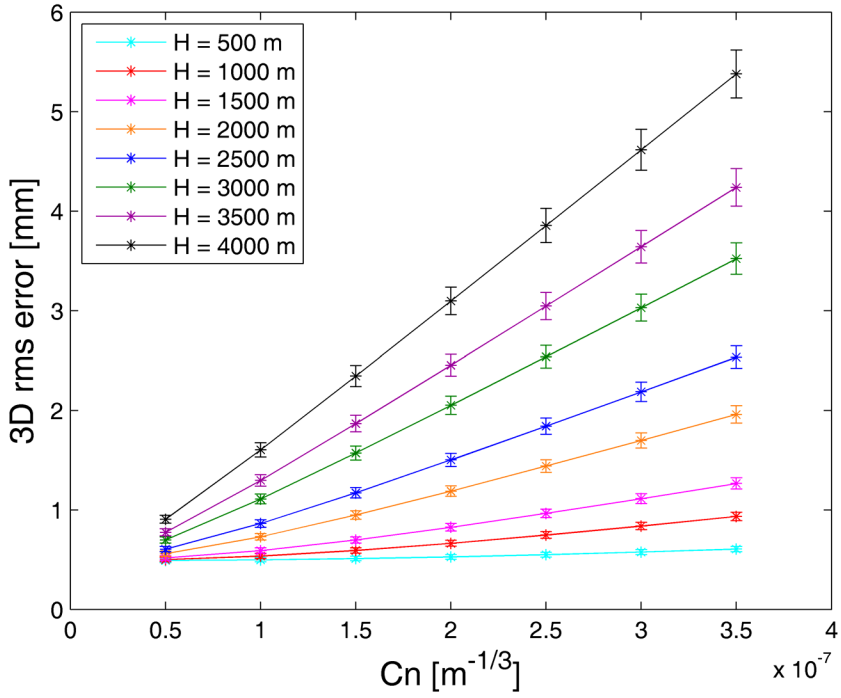

Figure 3: 3D rms error about the true error in mm versus refractive index structure constant C_n for different troposphere heights H. Wind speed: 7 m/s, the wind was blowing towards North-East. Schedule: st16uni_30_6_230X.skd, ASD 1e-14 @ 50 min, wn = 4/sqrt(2) ps. The error bars show 1 sigma of the rms scatter.

2.2 Varying the troposphere height *H*

Figure 4 shows rms about the true value of 3D position error for troposphere heights of 1000 (blue), 2000 (green) and 3000 (red) m. C_n was set to 1.0e-7 $m^{-1/3}$, v to 10 m/s. The error bars on top of the bars show 1 sigma of rms scatter (rms/sqrt(2n) where n is the number of repetitions, i.e. 25). It can be deduced from Figure 4 that also the effective height of the troposphere has a significant impact on position repeatability.

Table 2 shows the median 3D rms errors for the three runs with different heights. These values are plotted in Figure 5. The error bars in Figure 5 mark the 16th and 84th percentile, corresponding to 1 sigma about the median.

Table 2: median rms of 3D position error, Up, North, and East component for different values of H. C_n: 1.0 e-7 $m^{-1/3}$, v = 10 m/s, wind blowing towards East. Schedule_st16uni_60_12_230X.skd, ASD 1e-14 @ 50 min, wn = 4/sqrt(2) ps.

		H = 1000 m	H = 2000 m	H = 3000 m
median rms error [mm]	3D	0.8	1.0	1.4
	Up	0.8	0.9	1.3
	North	0.2	0.3	0.4
	East	0.2	0.2	0.3

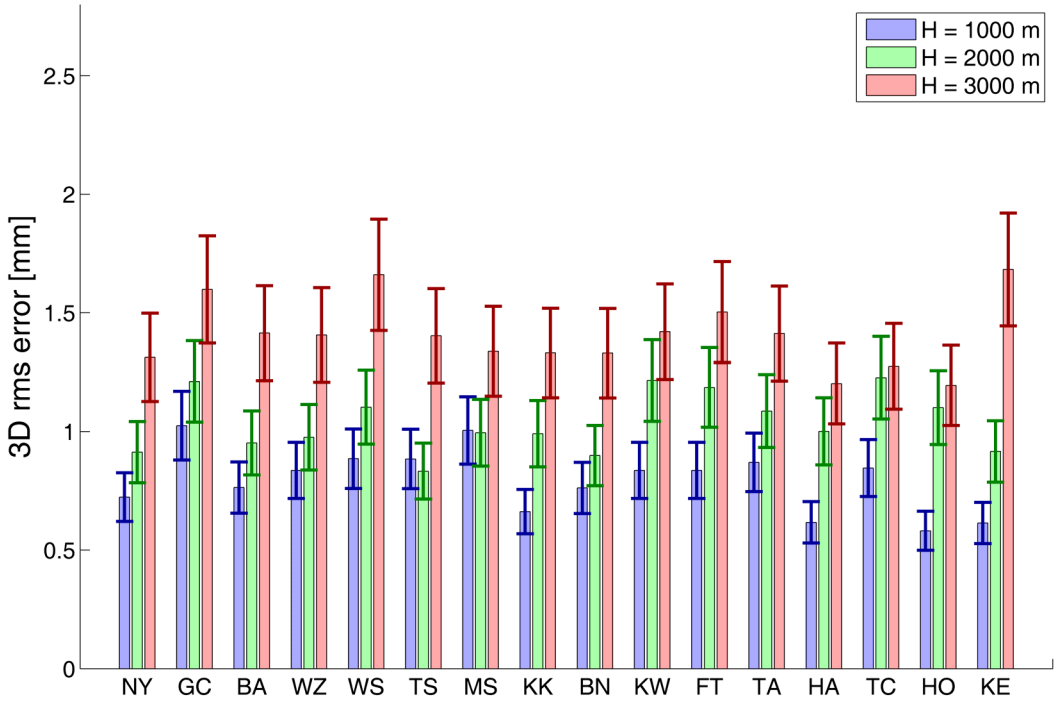

Figure 4: 3D rms error about the true value in mm for three different H values. C_n = 1.0 $m^{-1/3}$, v = 10 m/s, wind blowing towards East. For generation of the turbulent equivalent zenith wet delays the same parameters were used for all stations. Error bars: rms error/sqrt(2n), where n = 25. Schedule: st16uni_60_12_230X.skd, ASD 1e-14 @ 50 min, wn = 4/sqrt(2) ps.

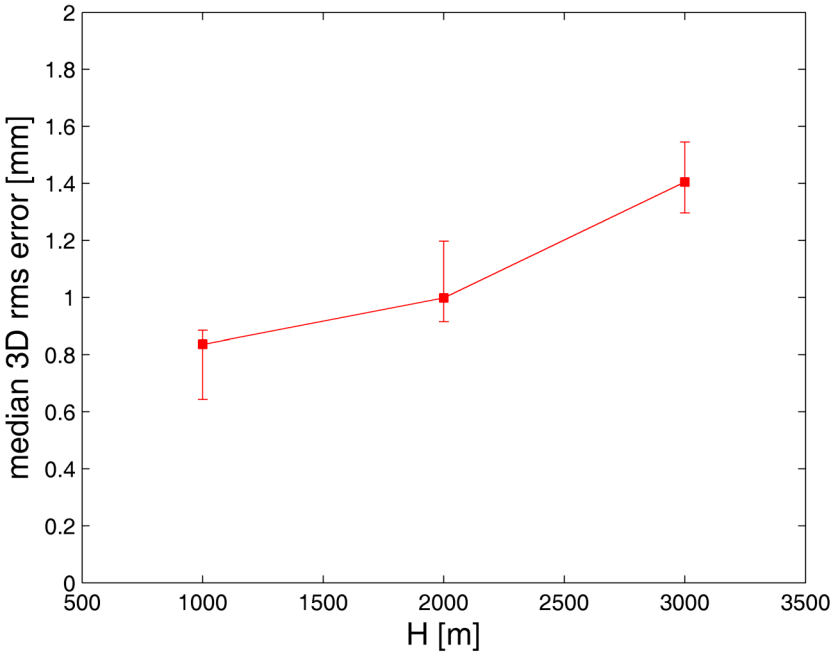

Figure 5: median 3D rms error [mm] versus troposphere height H. The errorbars show the 16th and 84th percentile, corresponding to 1 sigma about the median. Cn = 1.0e-7 $m^{-1/3}$, v = 10 m/s.

For station Wettzell, a more detailed investigation was carried out with the PPP Simulator. The results are presented in Figure 6 which shows 3D rms error versus troposphere height H for different values of C_n. The wind speed was chosen to be 7 m/s, the wind was blowing towards

North-East. The error bars show 1 sigma of the rms scatter (rms/sqrt(2n), where n is the number of repetitions, i.e. 250 for this investigation).

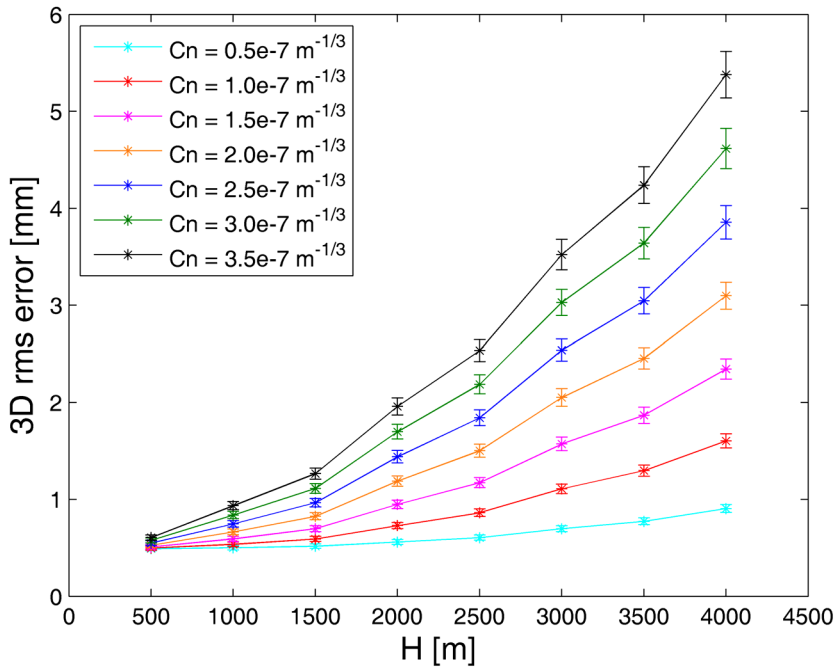

Figure 6: 3D rms error about the true value in mm versus troposphere height H for different refractive index structure constants C_n. Wind speed: 7 m/s, the wind was blowing towards North-East. Schedule: st16uni_30_6_230X.skd, ASD 1e-14 @ 50 min, wn = 4/sqrt(2) ps. The error bars show 1 sigma of the rms scatter.

2.3 Varying the wind speed v

Figure 7 shows the impact of the wind speed. 3D rms errors are plotted for wind speeds of 5, 10 and 20 m/s. C_n was 1.0e-7 $m^{-1/3}$, H was 2000 m. The wind was blowing towards East. The error bars on top of the bars show 1 sigma of rms scatter (rms/sqrt(2n) where n is the number of repetitions, i.e. 25). It can be seen that the 3D rms error is becoming worse with higher wind speed but that the impact of the wind is less significant than the impact of C_n and H.

The median 3D rms errors for the wind speeds tested are summarized in Table 3. These values are plotted versus wind speed in Figure 8. The error bars show the 16th and 84th percentile, corresponding to 1 sigma about the median.

Table 3: median rms of 3D position error, Up, North, and East component for different values of v. C_n: 1.0 e-7 $m^{-1/3}$, H = 2000 m, wind blowing towards East. Schedule: st16uni_60_12_230X.skd, ASD 1e-14 @ 50 min, wn = 4/sqrt(2) ps.

		v = 5 m/s	v = 10 m/s	v = 20 m/s
median rms error [mm]	3D	1.0	1.0	1.2
	Up	1.0	0.9	1.2
	North	0.3	0.3	0.3
	East	0.2	0.2	0.2

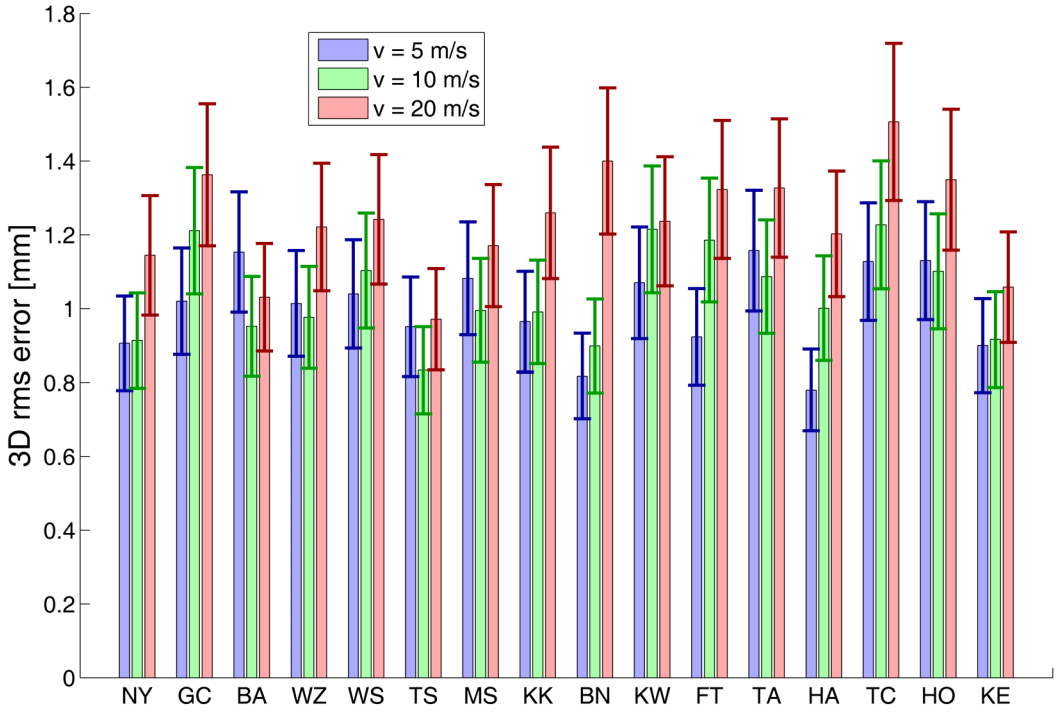

Figure 7: 3D rms error about the true value in mm for three different wind speeds. C_n = 1.0e-7 $m^{-1/3}$, H = 2000 m, wind blowing towards East. For generation of the turbulent equivalent zenith wet delays the same parameters were used for all stations. Error bars: rms error/sqrt(2n), where n = 25. Schedule: st16uni_60_12_230X.skd, ASD 1e-14 @ 50 min, wn = 4/sqrt(2) ps.

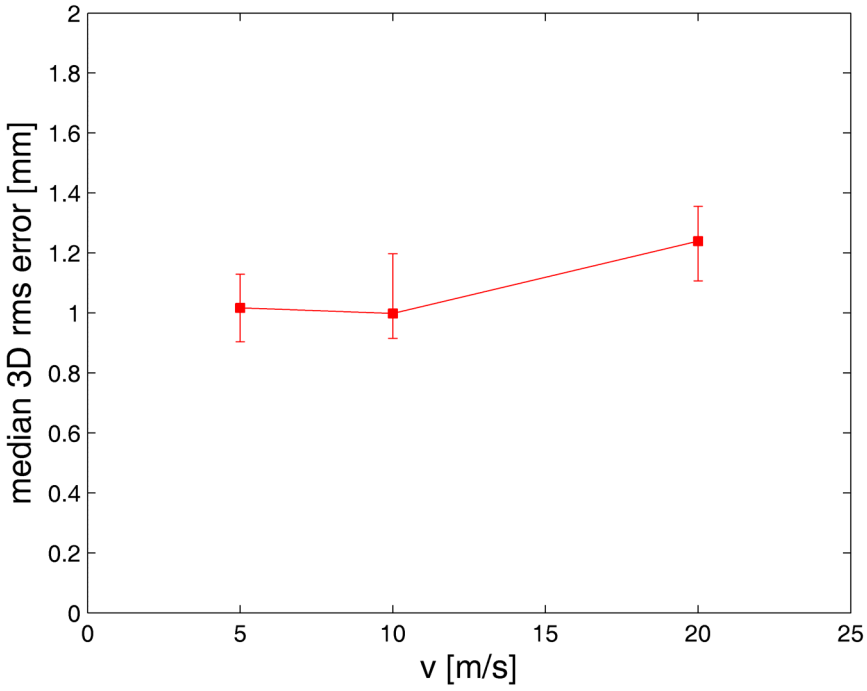

Figure 8: median 3D rms error [mm] versus wind speed v. The errorbars show the 16th and 84th percentile, corresponding to 1 sigma about the median. H = 2000 m, C_n = 1.0e-7 $m^{-1/3}$.

As for C_n and H, the investigation on the impact of the wind speed was carried out for station Wettzell for more combinations of C_n and H values (250 repetitions). Results can be seen in Figure 9 which shows 3D rms errors versus H for three different C_n values (0.5e-7 $m^{-1/3}$: red, 2.5e-7 $m^{-1/3}$: blue, 3.5e-7 $m^{-1/3}$: green) and two wind speeds (7 m/s: thick lines, 15 m/s: thin lines).

It can be deduced from this plot that the 3D rms error is becoming slightly worse with higher wind speed, when C_n and H are rather small, but that the 3D rms error is becoming better with higher wind speed, when C_n and H are rather high (compare also Wresnik et al. 2008).

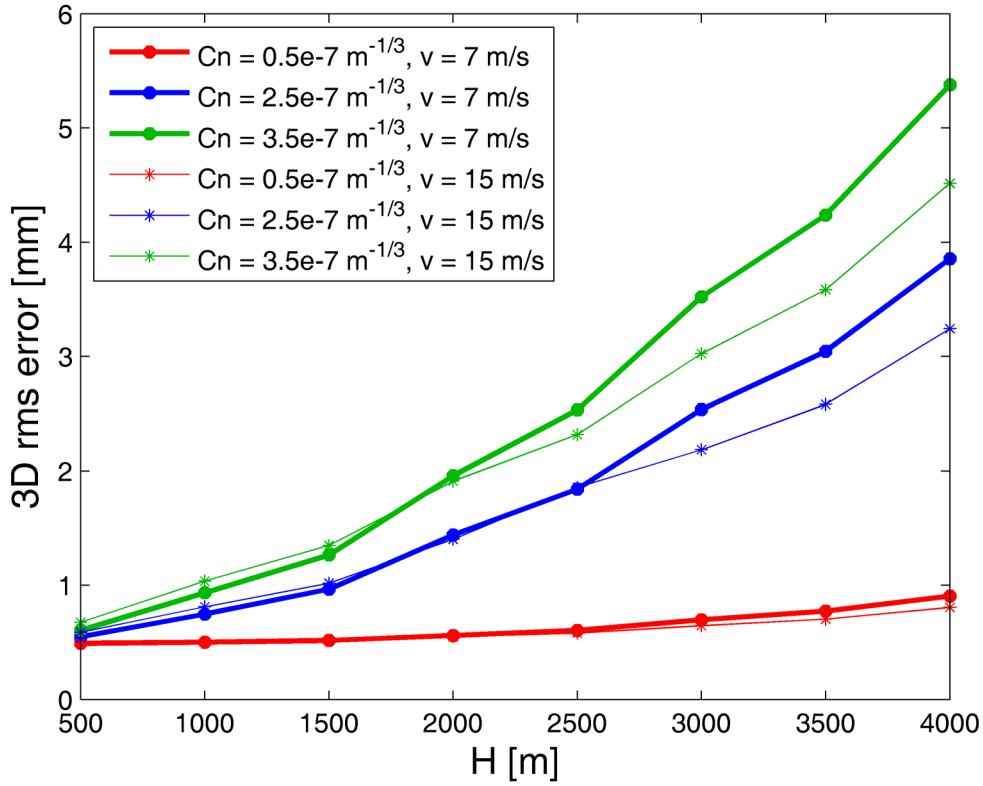

Figure 9: 3D rms error for three different C_n values versus H, using two different wind speeds. Schedule: st16uni_30_6_230X.skd, ASD 1e-14 @ 50 min, wn = 4/sqrt(2) ps.

2.4 Summary

Summarizing the investigation on the impact of turbulence parameters it can be said that the refractive index structure constant C_n and the troposphere height H have the most significant influence on position repeatability. The impact of wind speed is significantly smaller and dependent on the values of C_n and H: for small C_n and H the 3D rms error is the larger the higher the wind speed, for large C_n and H the 3D rms error is the smaller the higher the wind speed.

For the generation of turbulent equivalent zenith wet delays it is necessary to multiplicate with random numbers (see Nilsson et al. 2007). For the investigation on turbulence parameters, the same parameters have been used for all stations. The differences in 3D rms error between the stations are thus due to the multiplication with different sets of random numbers, and different realizations of station clock and white noise. Since former investigations have shown that the effect of station clock and white noise is pretty small, it can be stated that the main part of the scatter of the 3D rms errors (which can be deduced from Figures 1, 4 and 7) is due to the random numbers in the generation of turbulent equivalent zenith wet delays. The scatter is domianted by the choice of C_n and H.

3. Impact of clock accuracy

To investigate the impact of clock accuracy on station position repeatability, schedule st16uni_60_12_230.skd was run with 6 clocks with Allan standard deviations of 1e-15, 2e-15, 5e-15, 1e-14, 2e-14, 5e-14 @ 50 min. The turbulence parameters provided by Tobias Nilsson (see Appendix) were used for the generation of the turbulent equivalent zenith wet delays and a white noise (*wn*) of 4/sqrt(2) ps was added. The same zenith wet delay and *wn* time series were used for each of the clocks to make sure that the differences observed are due to the clock.

Figure 11 shows bar plots of 3D rms errors for the six different clocks. The upper plot shows results for the first 8 stations (order is North-South) and the lower plot for the second 8 stations. It can be deduced that for clocks with an ASD in the range between 1e-15 and 2e-14 @ 50 min there's not much sensitivity to clock accuracy.

Table 4 shows the median 3D rms errors for the six clocks. These values are plotted over clock accuracy in Figure 10. The errorbars show the 16th and 84th percentile, corresponding to 1 sigma about the median.

Table 4: median rms of 3D position error, Up, North, and East component for different clock accuracies. Schedule: st16uni_60_12_230X.skd, wn = 4/sqrt(2) ps, turbulence parameters as given in the appendix.

		ASD @ 50 min					
		1e-15	2e-15	5e-15	1e-14	2e-14	5e-14
median rms error [mm]	3D	1.2	1.2	1.2	1.4	1.7	2.9
	Up	1.1	1.1	1.1	1.3	1.6	2.8
	North	0.3	0.3	0.3	0.3	0.4	0.7
	East	0.2	0.3	0.3	0.3	0.3	0.6

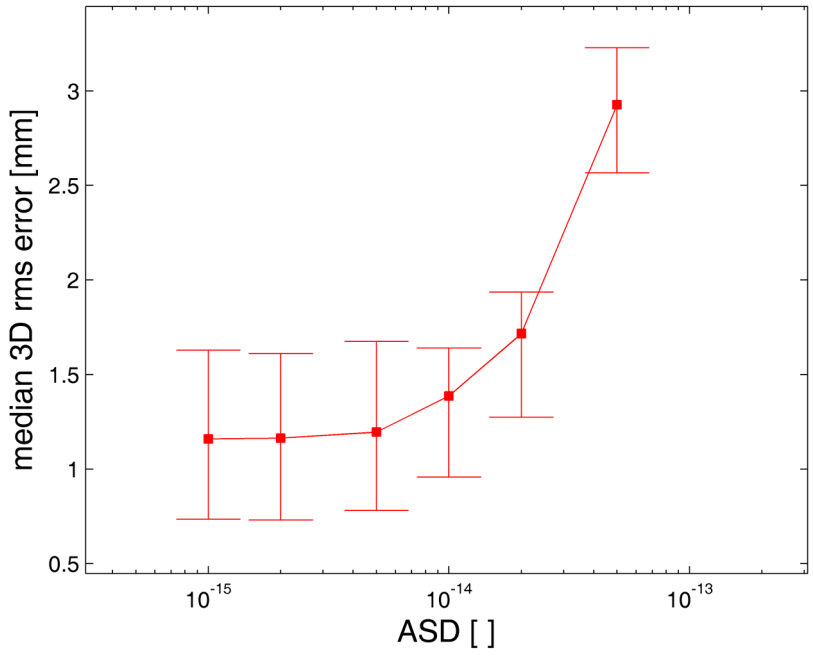

Figure 10: median 3D rms error versus clock accuracy. The errorbars show the 16th and 84th percentile, corresponding to 1 sigma about the median. Schedule: st16uni_60_12_230X.skd, wn = 4/sqrt(2) ps. Note that the scale of the x-axis is logarithmic.

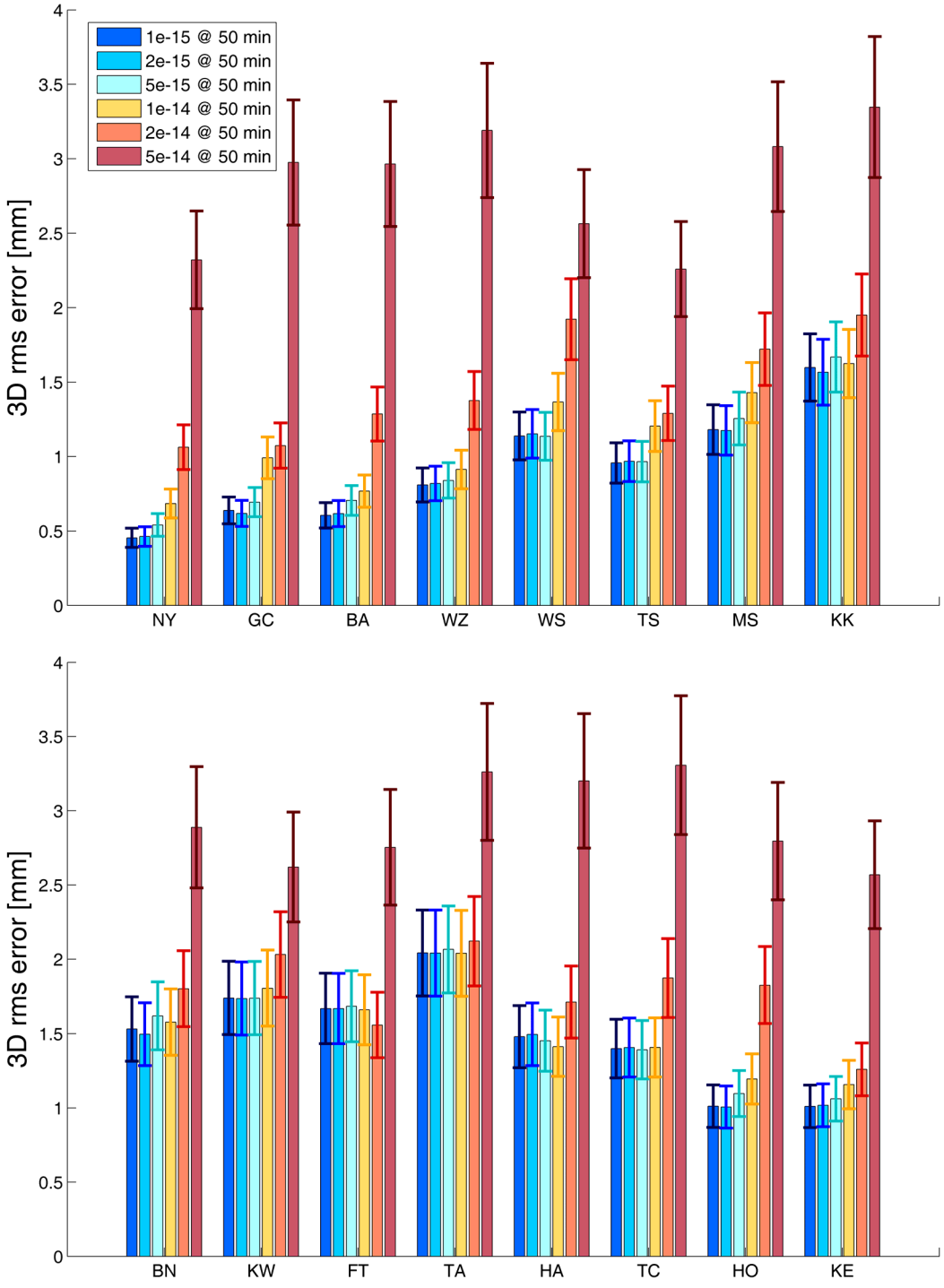

Figure 11: 3D rms errors for six different clocks. The same zenith wet delay and white noise time series were used for the six runs. Schedule: st16uni_60_12_230X.skd, turbulence parameters as given in the appendix, wn = 4/sqrt(2) ps. The error bars show 1 sigma of the scatter (rms/sqrt(2n), where n = 25).

4. Impact of thermal noise

To test the impact of thermal noise on position repeatability, runs with white noises of 4/sqrt(2), 8/sqrt(2), 12/sqrt(2), 16/sqrt(2), 24/sqrt(2), and 32/sqrt(2) ps were performed (schedule: st16uni_60_12_230X.skd, clock: 1e-14 @ 50 min). Figure 13 compares 3D rms error for the different white noises. The upper plot shows the first 8 stations, the lower plot the second 8 stations (station order is North-South). The differences in 3D rms errors are only due to the different white noises since the same troposphere and clock time series were used. A white noise of 32 ps is approximately what can be expected from the current VLBI system. A white noise of 4 ps is the nominal goal of VLBI 2010. The wn values are divided by sqrt(2) because single stations are evaluated instead of baselines. A wn of 4/sqrt(2) ps for PPP is equal to a wn of 4 ps in the OCCAM Simulator.

Table 5 shows the median 3D rms errors for the different white noises. These values are plotted over the white noise in Figure 12. The errorbars show the 16th and 84th percentile, corresponding to 1 sigma about the median.

Table 5: median rms of 3D position error, Up, North, and East component for different white noises. Schedule: st16uni_60_12_230X.skd, ASD 1e-14 @ 50 min, turbulence parameters as given in the appendix.

wn · sqrt(2)		4 ps	8 ps	12 ps	16 ps	24 ps	32 ps
median rms error [mm]	3D	1.3	1.5	1.7	1.7	2.6	3.0
	Up	1.2	1.4	1.6	1.7	2.5	2.8
	North	0.3	0.3	0.4	0.5	0.6	0.7
	East	0.3	0.3	0.4	0.4	0.5	0.7

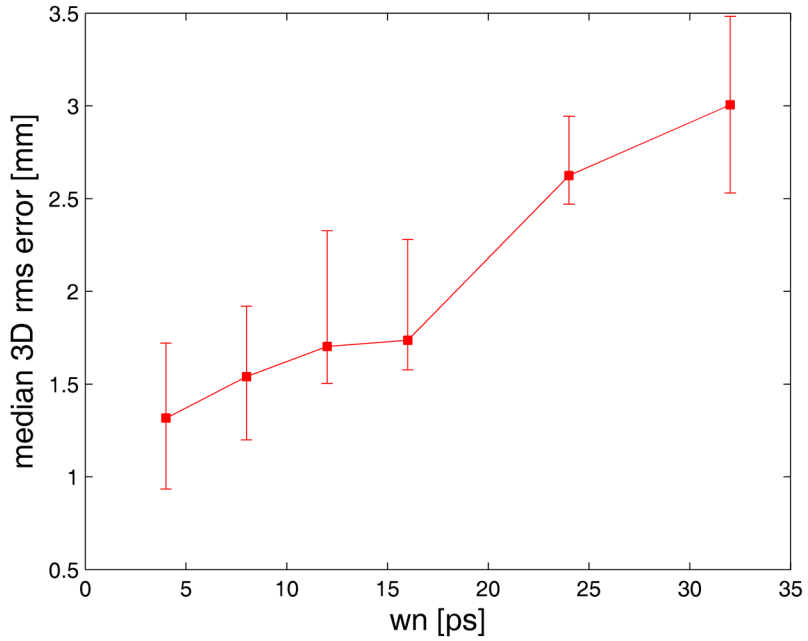

Figure 12: median 3D rms error versus white noise. The errorbars show the 16th and 84th percentile, corresponding to 1 sigma about the median. Schedule: st16uni_60_12_230X.skd, ASD 1e-14 @ 50 min.

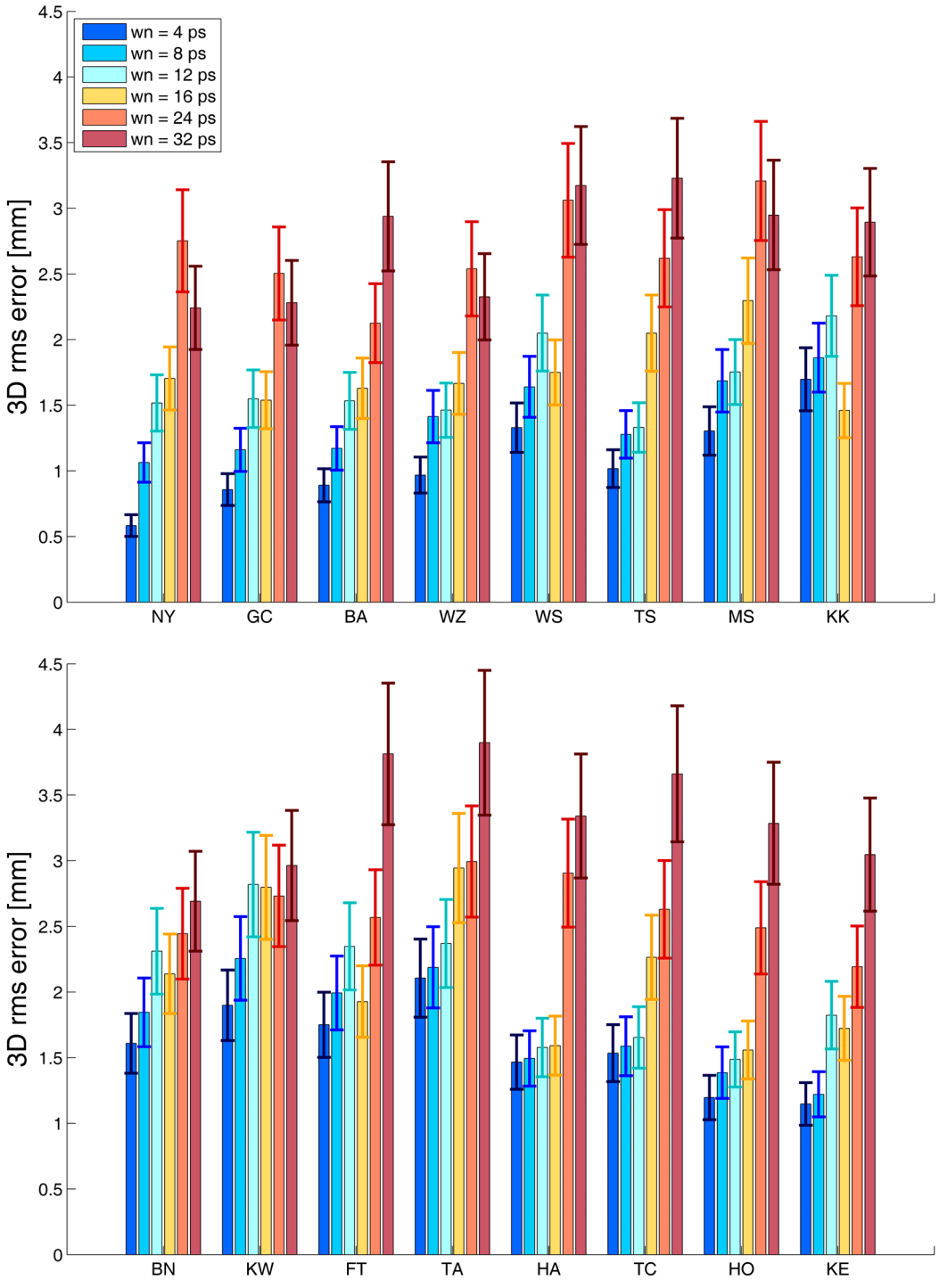

Figure 11: 3D rms errors for six different white noises. The same zenith wet delay and clock time series were used for the six runs. Schedule: st16uni_60_12_230X.skd, turbulence parameters as given in the appendix, ASD 1e-14 @ 50 min. The error bars show 1 sigma of the scatter (rms/sqrt(2n) where n = 25).

References:

Böhm, J., J. Wresnik, A. Pany, Simulation of wet zenith delays and clocks, IVS Memorandum 2006-013v03, 4 September 2007, http://ivscc.gsfc.nasa.gov/publications/memos/index.html, 2007

Nilsson, T., R. Haas, G. Elgered, Simulations of atmospheric path delays using turbulence models, In: Proceedings of the 18th European VLBI for Geodesy and Astrometry Working Meeting, 12-13 April 2007, edited by J. Böhm, A. Pany and H. Schuh, Geowissenschaftliche Mitteilungen, Heft Nr. 79, Schriftenreihe der Studienrichtung Vermessung und Geoinformation, Technische Universität Wien, ISSN 1811-8380, 175-180, 2007

Petrachenko, B., J. Böhm, D. MacMillan, A. Niell, A. Pany, A. Searle, J. Wresnik, VLBI2010 Antenna Slew Rate Study, submitted to the 5th IVS General Meeting Proceedings, 2008

Pany, A., J. Wresnik, J. Böhm, Vienna VLBI2010 PPP Simulator, IVS Memorandum, August 2008, http://ivscc.gsfc.nasa.gov/publications/memos/index.html, 2008

Wresnik, J., A. Pany, J. Böhm, Impact of Turbulence Parameters on VLBI2010 Simulation Results with OCCAM Kalman Filter, IVS Memorandum 2008-007v02, July 7 2008, http://ivscc.gsfc.nasa.gov/publications/memos/index.html, 2008

Wresnik, J., J. Böhm, H. Schuh, Monte Carlo Simulations for VLBI2010, In: Proceedings of the 18th European VLBI for Geodesy and Astrometry Working Meeting, 12-13 April 2007, edited by J. Böhm, A. Pany and H. Schuh, Geowissenschaftliche Mitteilungen, Heft Nr. 79, Schriftenreihe der Studienrichtung Vermessung und Geoinformation, Technische Universität Wien, ISSN 1811-8380, 168-174, 2007

Appendix:

# ST	Cn	H	vnor	veas
#	[$m^{-1/3}$]	[m]	[m/s]	[m/s]
BA	0.83	2410	0.25	4.74
BN	3.09	1788	3.46	-2.20
FT	1.80	2459	2.93	-7.12
GC	0.55	2079	3.80	-6.49
HA	2.02	2450	2.03	-2.84
HO	1.15	1804	3.03	11.14
KE	0.93	2569	3.40	17.50
KK	2.28	1477	4.38	-3.36
KW	3.06	1477	-1.64	-9.42
MS	1.90	1322	7.64	0.91
NY	0.35	2173	7.46	0.53
TA	2.66	2006	5.45	-1.17
TC	1.40	1869	1.21	4.96
TS	1.44	1767	1.03	10.49
WS	1.16	2887	5.39	11.88
WZ	0.93	2040	6.75	4.22